Supplemental material supporting "Understanding COVID-19 dynamics and the effects of interventions in the Philippines: A mathematical modelling study"

Jamie M. Caldwell PhD

Elvira de Lara-Tuprio PhD

Timothy Robin Teng PhD

Maria Regina Justina E. Estuar PhD

Raymond Francis R. Sarmiento MD

Milinda Abayawardana B.Eng

Robert Neil F. Leong MS

Richard T. Gray PhD

James G. Wood PhD

Emma S. McBryde PhD

Romain Ragonnet PhD

James Trauer PhD

Contents

1 Base model construction

1.1 Platform for infectious disease dynamics simulation

We developed a deterministic compartmental model of COVID-19 transmission using the AuTuMN platform, publicly available at https://github.com/monash-emu/AuTuMN/. This repository allows for the rapid and robust creation and stratification of models of infectious disease epidemiology and includes pluggable modules to simulate heterogeneous population mixing, demographic processes, multiple circulating pathogen strains, repeated stratification and other modelling features relevant to infectious disease transmission. The platform was created to simulate TB dynamics, being an infectious disease whose epidemiology differs markedly by setting, such that considerable flexibility is desirable [1]. We have progressively developed the structures of our platform over recent years, and further adapted it to be sufficiently flexible to permit simulation of other infectious diseases for the purpose of this project.

1.2 Base COVID-19 model

Using the base framework of an SEIR model (susceptible, exposed, infectious, removed), we split the exposed and infectious compartments into two sequential compartments each (SEEIIR). The two sequential exposed compartments represent the non-infectious and infectious phases of the incubation period, with the latter compartment representing the "presymptomatic" phase such that infectiousness occurs during three of the six sequential phases. For this reason, "active" is a more accurate term for the "I" compartments and is preferred henceforward. The two infectious compartments represent early and late phases of active disease and allow explicit representation of notification, case isolation, hospitalisation and admission to ICU. The "active" compartment also includes some persons who remain asymptomatic throughout their disease episode, such that this compartment does not map to either persons who are infectious or those who are diseased/symptomatic (Figure 1).

The latently infected and infectious presymptomatic periods together comprise the incubation period, with the incubation period and the proportion of this period for which patients are infectious defined by input parameters described below. In general, two sequential compartments can be used to form a gamma-

distributed profile of transition to infectiousness following exposure if the progression rates for these two compartments are equal, although in implementing this model the relative sojourn times in the two sequential compartments were not always identical. Nevertheless, this is broadly consistent with the empirically observed log-normal distribution of individual incubation periods [2].

The transition from early active to late active represents the point at which patients are detected (for those patients for whom detection does eventually occur) and isolation then occurs from this point forward (i.e. applies during the late disease phase only, see Section 2). This transition point is also intended to represent the point of admission to hospital or transition from hospital ward to intensive care for patients for whom this occurs (see Section 1.4).

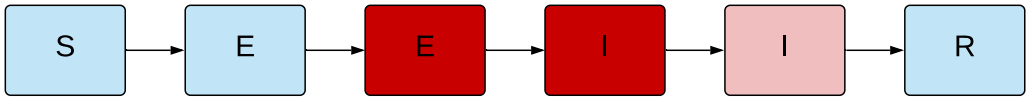

Figure 1 – Unstratified compartmental model structure. S = susceptible, E = exposed, I = active disease, R = recovered/removed.

Depth of pink/red shading indicates the infectiousness of the compartment.

1.3 Age stratification

All compartments of this base compartmental structure were stratified by age into five-year bands from 0-4 years of age through to 70-74 years of age, with the final age group being those aged 75 years and older. Heterogeneous baseline contact patterns by age were incorporated using age-specific contact rates estimated by Prem et al. 2017 [3], who combined survey response data with information on national demographic characteristics to produce age-structured mixing matrices with these age groupings. Our model age groups were chosen to match these mixing matrices. The automatic demographic features of AuTuMN that can be used to simulate births, ageing and deaths were not implemented, because the current questions at hand pertain to the short- to medium-term and the immediate implementation of non-pharmaceutical interventions,

for which population demographics are less relevant.

1.4 Clinical stratification

The age-stratified late exposed/incubation and both the early and late active disease compartments are further stratified into five categories: *1)* asymptomatic, *2)* symptomatic ambulatory, never detected, *3)* symptomatic ambulatory, ever detected, *4)* ever hospitalised, never critical and *5)* ever critically unwell (Figure 2). The proportion of new infectious persons entering stratum 1 (asymptomatic) is age-dependent (as described in Table 4). The proportion of symptomatic patients (strata 2 to 5) ever detected (strata 3 to 5) is set through a parameter that represents the time-varying proportion of all symptomatic patients who are ever detected (the case detection rate, see Section 2). Of those ever symptomatic (strata 2 to 5), a constant but age-specific proportion is considered to be hospitalised (entering strata 4 or 5). Of those hospitalised (entering strata 4 or 5), a fixed proportion was considered to be critically unwell (entering stratum 5, Figure 3).

1.5 Hospitalisation

For COVID-19 patients who are admitted to hospital, the sojourn time in the early and late active compartments is modified, overwriting the sojourn times the default values for these compartments, as indicated in Table 3. The point of admission to hospital is considered to be the transition from early to late active disease, such that the sojourn time in late disease is the period of time admitted to hospital. For patients admitted to ICU, admission to ICU occurs at this same transition point. For this group, the period of time hospitalised outside of ICU is estimated as a proportion of the early active period, such that the early active period represents both the period ambulatory in the community and the period in hospital prior to ICU admission.

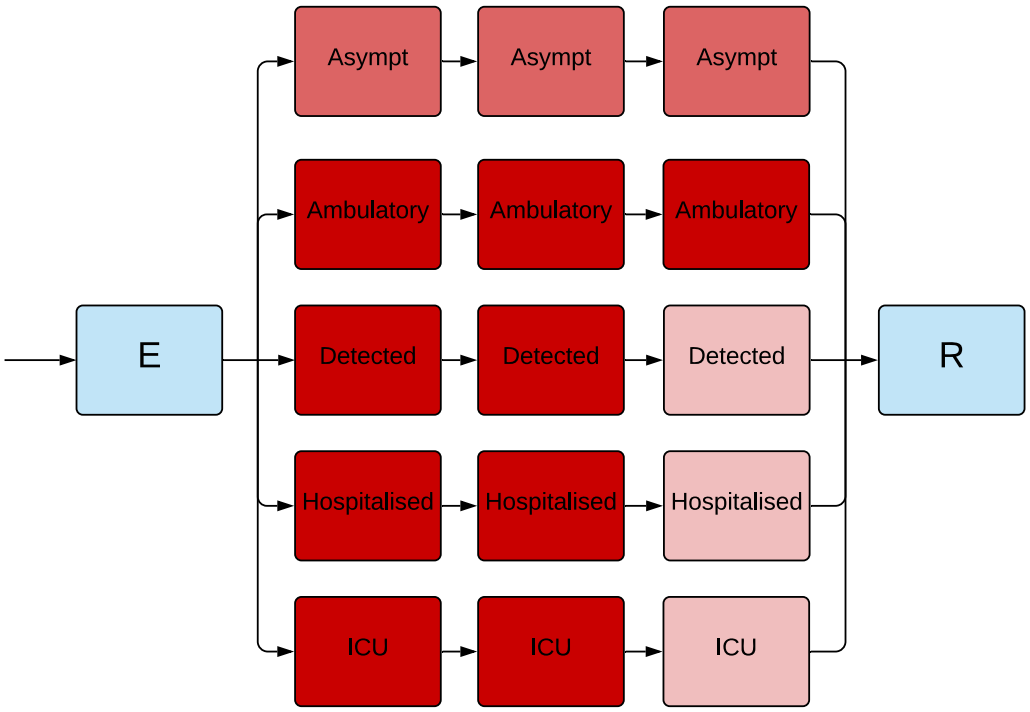

Figure 2 – Illustration of the implementation of the clinical stratification.

Depth of pink/red shading indicates the infectiousness of the compartment.

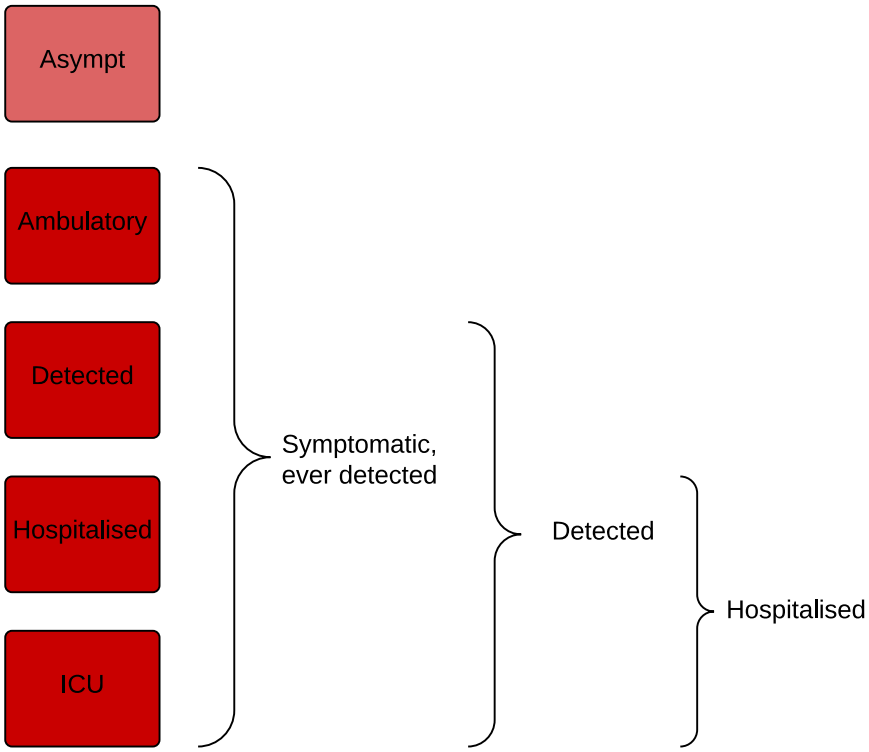

Figure 3 – Illustration of the rationale for the clinical stratification.

1.6 Infectiousness

The relative infectiousness of both early and late compartments within the asymptomatic stratum is modified to reflect lower infectiousness per unit time undiagnosed for asymptomatic persons. Presymptomatic individuals are assumed to have the same level of infectiousness as symptomatic diseased individuals. A proportion of COVID-19 patients who have been detected by the public health systems are assumed to self-isolate from the point of entering the late disease compartment, reducing the infectiousness of this group. Infectiousness declines at the point of transition from early to late disease for all patients admitted to hospital (both ICU and non-ICU) to reflect hospital infection control.

1.7 Application of COVID-19-related death

Age-specific infection fatality rates (IFRs) were applied and distributed across strata 4 and 5, with no deaths typically applied to the first three strata. A ceiling of 50% is set on the proportion of those admitted to ICU (entering stratum 5) who can die. If the infection fatality rate is greater than this ceiling, the proportion of critically unwell persons dying was set to one half, with the remainder of the infection fatality rate then applied to the hospitalised proportion. Otherwise, if the infection fatality rate is less than half of the absolute proportion of persons critically unwell, the infection fatality rate is applied entirely through stratum 5 (such that the proportion of critically unwell persons dying in that age group becomes $<$50% and the proportion of stratum 4 dying is set to zero). In the event that the infection fatality rate for an age group is greater than the total proportion hospitalised (which is unusual, but could occur for the oldest age group under certain parameter configurations), the remaining deaths are assigned to the asymptomatic stratum. This approach was chosen because this stratum has a fixed value over time and the dynamics are equivalent to assigning the deaths to any of the first three strata, because the sojourn times in the infected compartments are the same for each of these groups. We used the age-specific IFRs previously estimated from age-specific death data from 45 countries and results from national-level seroprevalence surveys [4]. We allowed IFRs to vary around the previously published point estimates in order to incorporate uncertainty and to allow IFRs to vary by country (see Calibration section).

Clinical stratum	Stratum name	Pre-symptomatic	Early	Late
1	Asymptomatic	0.5	0.5	0.5
2	Symptomatic ambulatory never detected	1	1	1
3	Symptomatic ambulatory ever detected	1	1	0.2
4	Hospitalised never critical	1	1	0.2
5	Ever critically unwell	1	1	0.2

Table 1 – Illustration of the relative infectiousness of disease compartments by clinical stratification and stage of infection.

2 Case detection rate

2.1 General approach

We calculate a time-varying case detection rate, being the proportion of all symptomatic cases (clinical strata 2 to 5) that are detected (clinical strata 3 to 5). This proportion is informed by the number of tests performed using the following formula:

$$CDR(time) = 1 - e^{-shape \times tests(time)}$$

time is the time in days from the 31st December 2019 and *tests(time)* is the number of tests per capita done on that date. To determine the value of the shape parameter, we solve this equation based on the assumption that a certain daily testing rate *tests(time)* is associated with a certain *CDR(time)*. Solving for *shape* yields:

$$shape = \frac{-log(1 - CDR(time))}{tests(time)}$$

That is, if it is assumed that a certain daily per capita testing rate is associated with a certain proportion of symptomatic cases detected, we can determine *shape*. As this relationship is not well understood and unlikely to be consistent across all settings, we routinely vary the *CDR* that is associated with a certain per capita testing rate during uncertainty/calibration. Given that the *CDR* value can be varied widely, the

purpose of this is to incorporate changes in the case detection rate that reflect real historical profile in changes in testing capacity over time.

3 Implementation of non-pharmaceutical interventions

A major part of the rationale for the development of this model was to capture the past impact of non-pharmaceutical interventions (NPIs) and produce future scenarios projections with the implementation or release of such interventions.

3.1 Isolation and quarantine

For persons who are identified with symptomatic disease and enter clinical stratum 3, self-isolation is assumed to occur and their infectiousness is modified, as described above. The proportion of ambulatory symptomatic persons effectively identified through the public health response by any means is determined by the case detection rate as described above.

3.2 Community quarantine or "lockdown" measures

For all NPIs relating to reduction of human mobility or "lockdown" (i.e. all NPIs other than isolation and quarantine mentioned above), these interventions are implemented through dynamic adjustments to the age-assortative mixing matrix. The mixing matrices of Prem et al. [3] are synthetic and do not represent direct observations or reports from surveys (in the case of the 144 countries to which they were extrapolated from observations in the eight "POLYMOD" countries of Western Europe). In addition, the code and methodology used to derive these matrices is not publicly available or presented in such a way to allow reproduction of their methods. Nevertheless, the matrices are contextualised to local demographic information for each country, including country-specific data that include household size, workforce participation and school enrolment. Further, the matrices presented are easily machine-readable and appear to be plausible representations of contact structures within these countries. New mixing matrices have recently been developed by the same group and are available as a pre-print. These are likely to represent an improvement on the previous matrices and will be incorporated into our framework at such time as they they reach publication.

The matrices also have the major advantage of allowing for disaggregation of total contact rates by location, i.e. home, work, school and other locations. This disaggregation allows for the simulation of various NPIs in a local context by dynamically varying the contribution of each location to reflect the historical implementation of the interventions.

The corresponding mixing matrix (denoted C_0) is presented for each individual model application, using the standard convention that a row represents the average numbers of age-specific contacts per day for a contact recipient of a given age-group. In other words, the element $C_{0i,j}$ is the average number of contacts per day that an individual of age-group $_i$ has with individuals of age-group $_j$.

This matrix results from the summation of the four context-specific contact matrices provided by Prem et al.: $C_0 = C_H + C_S + C_W + C_L$, where C_H, C_S, C_W and C_L are the age-specific contact matrices associated with households, schools, workplaces and other locations, respectively.

In our model, the contributions of the matrices C_S, C_W and C_L vary with time such that the input contact matrix can be written:

$$C(t) = h(t) \times C_H + s(t) \times C_S + w(t) \times C_W + l(t) \times C_L$$

3.3 School closures/re-openings

Complete school closures are represented by entirely removing the contribution of the school-based contacts to the mixing matrix at the point of school closures and re-instating them when schools reopen (that is applying a smoothed step function such that C_S becomes zero). Note that this complete removal or re-instatement of this contribution to the mixing matrix is a more dramatic change than is seen with the simulation of policy changes in workplaces and other locations.

3.4 Workplace closures

Workplace closures are presented by proportionally reducing the contribution of workplace contacts to the total mixing matrix over time. The profile of this reduction is set by fitting a spline function to Google mobility data.

3.5 Community-wide movement restriction

This is simulated by reducing the contribution of the "other locations" contacts to the overall mixing matrix. The functional form of this reduction is set by fitting a function of time to the relative change in the values of Google mobility data compared to baseline/pre-pandemic levels.

Prem "location"	**Approach**	**Google mobility types**
School	Policy response	Not applicable
Household	Google mobility	Residential
Workplace	Google mobility	Workplace
Other locations	Google mobility	Unweighted average of: • Retail and recreation • Grocery and pharmacy • Parks • Transit stations

Table 2 – Mapping of Google mobility data to contact locations (as defined by Prem et al.)

3.6 Microdistancing

For several applications of this model, it was found that the adaptations to the mixing matrices described above were insufficient to capture the full extent of the improvements in epidemiology as NPIs were implemented. We therefore implemented a "microdistancing" function to represent a reduction in the rate of contact in locations outside of the household that is not captured through Google mobility data. The microdistancing function reduces the values of all elements of the mixing matrices by a certain proportion (although functionality exists for this to be applied to certain locations only).

To parameterise this process, a function of time was developed for each setting that represents the historical policy changes implemented, which is typically set to a maximum value of one, such that the values represent the proportion of the maximum effect achieved by each set of restrictions. This enables a single parameter (the maximum effect of microdistancing) to be calibrated to reflect the maximum impact of policy changes on microdistancing, while the relative effect of each change is fixed and estimated from

available evidence.

4 Parameters

Parameter	Value	Rationale
Incubation period	Calibration parameter, truncated normal distribution, mean 5.5 days	Estimates of the incubation period have included 5.1 days, 5.2 days and 4.8 days [5] [6] [7] [8]. A systematic review [2] found that data are best fitted by a log-normal distribution (mean 5.8 days, CI 5.0 to 6.7, median 5.1 days). Our systematic review [9] found that estimates of the mean incubation period have varied from 3.6 to 7.4 days.
Proportion of incubation period infectious	50%	Infectiousness is considered to be present throughout a considerable proportion of the incubation period, based on analyses of confirmed source-secondary pairs [10] and early findings that the incubation period was similar to the serial interval [5]. The study of source-secondary pairs was also the primary reference cited by a review of the infectious period that identified studies that quantified the pre-symptomatic period, which concluded that the median pre-symptomatic period could range from less than one to four days [11].
Active period (regardless of detection/isolation, for clinical strata 1 to 3)	Calibration parameter, truncated normal distribution, mean 8 days	This quantity is difficult to estimate, given that identified cases are typically quarantined. Studies in settings of high case ascertainment and an effective public health response have suggested a duration of greater than 5.5 days [8]. PCR positivity, which may continue for up to two to three weeks from the point of symptom onset [10] [11], is difficult to interpret and does not necessarily indicate infectiousness. Consistent with these findings, the duration infectious for asymptomatic persons has been estimated at 6.5 to 9.5 days [11] (although in our model, this would include the pre-symptomatic infectious period).
Proportion of infectious period before isolation or hospitalisation can occur	0.33	Assumed

Continuation of Table 3

Parameter	Value	Rationale
Disease duration prior to admission for hospitalised patients not critically unwell (i.e. early active sojourn time, stratum 4)	7.7 days	Mean value from ISARIC cohort, as reported on 4th October 2020 in Table 6 [12], and similar to the expected mean from earlier reports from ISARIC [13]. This cohort represents high-income countries better than low and middle-income countries, with the United Kingdom contributing data on the greatest number of patients, followed by France. Earlier estimates of this quantity from China included 4.4 days [5].
Duration of hospitalisation if not critically unwell (late active sojourn time, stratum 4)	12.8 days	Mean value from the ISARIC cohort, as reported on 4th October 2020 in Table 6 [12].
ICU duration (late active sojourn time, stratum 5)	10.5 days	Mean duration of stay in ICU/HDU from ISARIC cohort for patients with complete data, as reported on 10th October 2020 Table 6 [12]. Many other studies reporting on the average duration of ICU stay suffer from right-truncation issues, often estimating 7-10 days length of stay.
Duration of time prior to ICU for patients admitted to ICU	10.5 days	Calculated as the sum of the time from symptom onset to hospital admission (7.7 days above) plus the duration from hospital admission to ICU admission reported by October ISARIC report (2.8 days) [12].
Relative infectiousness of asymptomatic persons (per unit time with active disease)	0.5	Assumed
Relative infectiousness of persons admitted to hospital or ICU	0.2	Assumed
Relative infectiousness of identified persons in isolation	0.2	Assumed
Proportion of hospitalised patients ever admitted to ICU	0.17	Assumed

Table 3 – **Universal (non-age-stratified) model parameters.** Point estimates are used as model parameters except where ranges are indicated in calibration parameter table below in calibration table

Age group (years)	Clinical fraction[a]	Relative susceptibility to infection	Infection fatality rate	Proportion of symptomatic patients hospitalised
0 to 4	0.29	0.36	3×10^{-5}	0.0777
5 to 9	0.29	0.36	1×10^{-5}	0.0069
10 to 14	0.21	0.36	1×10^{-5}	0.0034
15 to 19	0.21	1	3×10^{-5}	0.0051
20 to 24	0.27	1	6×10^{-5}	0.0068
25 to 29	0.27	1	1.3×10^{-4}	0.0080
30 to 34	0.33	1	2.4×10^{-4}	0.0124
35 to 39	0.33	1	4.0×10^{-4}	0.0129
40 to 44	0.40	1	7.5×10^{-4}	0.0190
45 to 49	0.40	1	1.21×10^{-3}	0.0331
50 to 54	0.49	1	2.07×10^{-3}	0.0383
55 to 59	0.49	1	3.23×10^{-3}	0.0579
60 to 64	0.63	1	4.56×10^{-3}	0.0617
65 to 69	0.63	1.41	1.075×10^{-2}	0.1030
70 to 74	0.69	1.41	1.674×10^{-2}	1.072
75 and above	0.69	1.41	5.748×10^{-2}, [b]	0.0703
Source/ rationale	Model fitting to age-distribution of early cases in China, Italy, Japan, Singapore, South Korea and Canada taken from upper-left panel of Figure 2b of [14].	Conversion of odds ratios presented in Table S15 of Zhang et al. 2020 to relative risks using data presented in Table S14 of the same study [15].[c]	Estimated from pooled analysis of data from 45 countries from Table S3 of O'Driscoll et al [4]. Values consistent with previous estimates using serosurveys performed in Spain [16].	Estimates from the Netherlands as the first wave of infections declined from 4th May to 21st July [17].

Table 4 – **Age-stratified parameter values.** Age-stratified parameters not varied during calibration, or varied through a common multiplier.
[a] Proportion of incident cases developing symptoms.
[b] Weighted average of IFR estimates for 70 to 79 and 80 and above age groups.
[c] Note the relative magnitude of these values are similar to those estimated by the analysis we use to estimate the age-specific clinical fraction.[14]

5 Calculation of outputs

5.1 Incidence

Incidence is calculated as transitions from the late exposed compartment (*"E"*) to the early active compartment (*"I"*). This only applies to locally-transmitted cases and so does not include importations.

5.2 Hospital occupancy

This is calculated as the sum of three quantities:

1. All persons in the late active compartment in clinical stratum 4, representing those admitted to hospital but never critically unwell.

2. All persons in the late active compartment in clinical stratum 5, representing those currently admitted to ICU.

3. A proportion of the early active compartment in clinical stratum 5, representing those who will be admitted to ICU at a time in the future. This proportion is calculated as the quotient of *1)* the difference between the pre-ICU period and the pre-hospital period for clinical stratum 4, divided by *2)* the total pre-ICU period. That is, a proportion of the pre-ICU period is considered to represent patients in hospital who have not yet been admitted to ICU.

5.3 ICU occupancy

This is calculated as all persons in the late active compartment in clinical stratum 4.

5.4 Seropositive proportion

This is calculated as the proportion of the population in the recovered or "R" compartment.

5.5 COVID-19-related mortality

This is calculated as all transitions representing death, exiting the model. This is implemented as depletion of the late active compartment.

5.6 Notifications

Local case notifications are calculated as transitions from the early to the late active compartment for clinical strata 3 to 5. Imported case notifications are calculated as the product of the time-variant importation rate (which has been inflated for incomplete case detection) and the case detection rate.

6 Calibration

6.1 General approach

The model was calibrated using an adaptive Metropolis (AM) algorithm. In particular, we used the algorithm based on adaptive Gaussian proposal functions proposed by Haario *et al.* to sample parameters from their posterior distributions [18]. For each application, we run seven independent AM chains initialised using Latin Hypercube Sampling across the uncertainty parameters being calibrated. The number of iterations was limited by a maximum computational time, typically of one to two hours per chain. We discarded the first 200 iterations of each chain as burn-in and combined the samples of the seven chains to project epidemic trajectories over time. The definitions of the prior distributions and the likelihood are detailed below.

6.2 Likelihood function

Likelihood functions are derived from comparing model outputs to target data at each time point nominated for calibration. The standard deviations of this distribution are considered as calibration parameters and varied during the calibration approach to improve calibration efficiency.

6.3 Variation of infection fatality rate and symptomatic proportions

Whether age-specific infection fatality rates (IFRs) are significantly different in low- and middle-income settings from those in high-income settings remains highly uncertain. For this application to the Philippines, we adjust the IFRs described above according to a factor that modifies the age-specific IFR for each age group relative to the baseline values described in the previous section, allowing them to vary from those reported up to two-fold those values. The age-specific IFRs used in the model are obtained from:

$$IRF_i^* = \frac{IFR_i \times \omega}{IFR_i(\omega - 1) + 1},$$

where IRF_i^* is the modelled IFR for age group i, IFR_i is the point estimate reported by O'Driscoll *et al.* for the IFR of age group i [4], and ω is the uncertainty adjuster varied during model calibration.

Similarly, we incorporated uncertainty around the age-specific proportions of symptomatic individuals by applying an uncertainty adjuster:

$$s_i^* = \frac{s_i \times \gamma}{s_i(\gamma - 1) + 1},$$

where s_i^* is the modelled symptomatic proportion for age group i, s_i is the point estimate reported by Davies *et al.* for the IFR of age group i [14], and γ is the associated uncertainty adjuster varied during model calibration.

6.4 Calibration parameters

Parameter name	**Distribution type**	**Distribution parameters**
Incubation period	Truncated normal	Mean 5.5 days, standard deviation 0.97 days, truncation $<$1 day
Infectious period (for clinical strata 1 to 3)	Truncated normal	Mean 6.5 days, standard deviation 0.77 days, truncation $<$4 days
Risk of infection per contact	Uniform	0.03 to 0.05
Infection fatality rate adjuster (ω)	Uniform	Range 1.8 to 2.28

Continuation of Table 5

Parameter name	**Distribution type**	**Distribution parameters**
Proportion of symptomatic cases that would be detected with a daily per capita testing rate of one test per ten thousand population	Uniform	Range 0.02 to 0.15
Infectious seed	Uniform	Range 10 to 100
Maximal effect of Minimum Health Standards	Uniform	0.1 to 0.6
Adjuster applied to age-specific proportion of infections leading to symptoms (“Clinical fraction”)	Truncated normal	Mean 1, standard deviation 0.2, truncation $<$0.5

Table 5 – Epidemiological calibration parameters.

6.5 Calibration targets

We calibrated each of the Philippines models to the daily notification rate (with seven-day moving average smoothing) observed nationally or for the sub-region simulated over time.

For ICU occupancy, we only considered the most recent estimate of ICU occupancy and did not calibrate to multiple time points for this indicator. Similarly for cumulative infection-related deaths, we only calibrated to the most recent data time point available.

7 Supplemental figures and tables to main text

7.1 Supplemental Tables

Table 6 – Laboratory testing facilities by region.

Facility Name	Region
Batangas Medical Center GeneXpert Laboratory	Calabarzon
Daniel O. Mercado Medical Center	Calabarzon
De La Salle Medical and Health Sciences Institute	Calabarzon
Greencity Medical Center	Calabarzon
Lucena United Doctors Hospital and Medical Center	Calabarzon
Mary Mediatrix Medical Center	Calabarzon
Ospital ng Imus	Calabarzon
Qualimed Hospital Sta. Rosa	Calabarzon
San Pablo College Medical Center	Calabarzon
San Pablo District Hospital	Calabarzon
UPLB Covid-19 Molecular Laboratory	Calabarzon
Allegiant Regional Care Hospital	Central Visayas
Cebu Doctors University Hospital Inc	Central Visayas
CebuTBReferenceLaboratory-MolecularFacilityforCOVID-19Testing	Central Visayas
Chong Hua Hospital	Central Visayas

Facility Name	**Region**
Governor Celestino Gallares Memorial Medical Center	Central Visayas
Prime Care Alpha Covid-19 Testing Laboratory	Central Visayas
University of Cebu Medical Center	Central Visayas
Vicente Sotto Memorial Medical Center (VSMMC)	Central Visayas
Amang Rodriguez Memorial Center GeneXpert Laboratory	National Capital Region
Asian Hospital and Medical Center	National Capital Region
Chinese General Hospital	National Capital Region
De Los Santos Medical Center	National Capital Region
Dr. Jose N. Rodriguez Memorial Hospital and Sanitarium (TALA) GeneXpert Laboratory	National Capital Region
Dr. Jose N. Rodriguez Memorial Hospital and Sanitarium (TALA) RT PCR	National Capital Region
Fe del Mundo Medical center	National Capital Region
Hi-Precision Diagnostics (QC)	National Capital Region
Lung Center of the Philippines (LCP)	National Capital Region
Lung Center of the Philippines GeneXpert Laboratory	National Capital Region
Makati Medical Center (MMC)	National Capital Region
Marikina Molecular Diagnostics Laboratory (MMDL)	National Capital Region
National Kidney and Transplant Institute	National Capital Region
National Kidney and Transplant Institute GeneXpert Laboratory	National Capital Region

Facility Name	Region
Philippine Children's Medical Center	National Capital Region
Philippine Heart Center GeneXpert Laboratory	National Capital Region
SafeguardDNADiagnosticsInc	National Capital Region
San Miguel Foundation Testing Laboratory	National Capital Region
Singapore Diagnostics	National Capital Region
St. Luke's Medical Center - BGC (HB) GeneXpert Laboratory	National Capital Region
St. Luke's Medical Center - BGC (SLMC-BGC)	National Capital Region
St. Luke's Medical Center - Quezon City (SLMC-QC)	National Capital Region
Sta. Ana Hospital - Closed System Molecular Laboratory (GeneXpert)	National Capital Region
The Medical City (TMC)	National Capital Region
Tondo Medical Center GeneXpert Laboratory	National Capital Region
Tropical Disease Foundation	National Capital Region
University of Perpetual Help DALTA Medical Center Inc	National Capital Region
UP-PGH Molecular Laboratory	National Capital Region
UP National Institutes of Health (UP-NIH)	National Capital Region
UP Philippine Genome Center	National Capital Region
Veteran Memorial Medical Center	National Capital Region
Victoriano Luna - AFRIMS	National Capital Region

7.2 Supplemental Figures

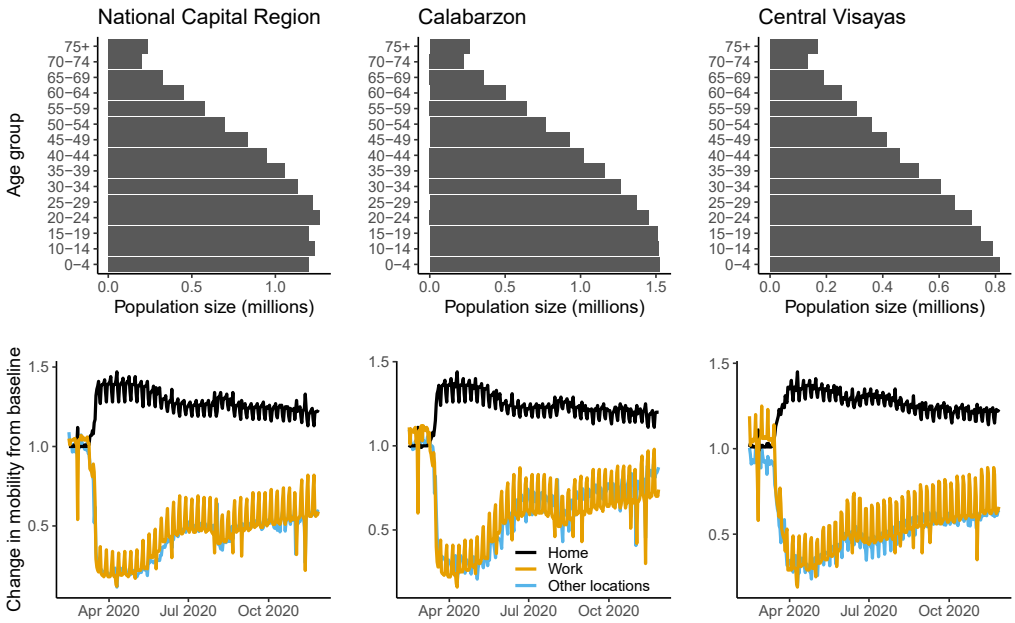

Figure 4 – Population size and mobility included in the age-structured COVID-19 for three regions of the Philippines. Starting population age distribution (top row) and community quarantine driven mobility adjustments applied to the mixing matrices (bottom row) for Calabarzon (left), Central Visayas (middle), and the National Capital Region (right). Other locations in the mobility plots include retail and recreation, supermarket and pharmacy, parks, and public transport.

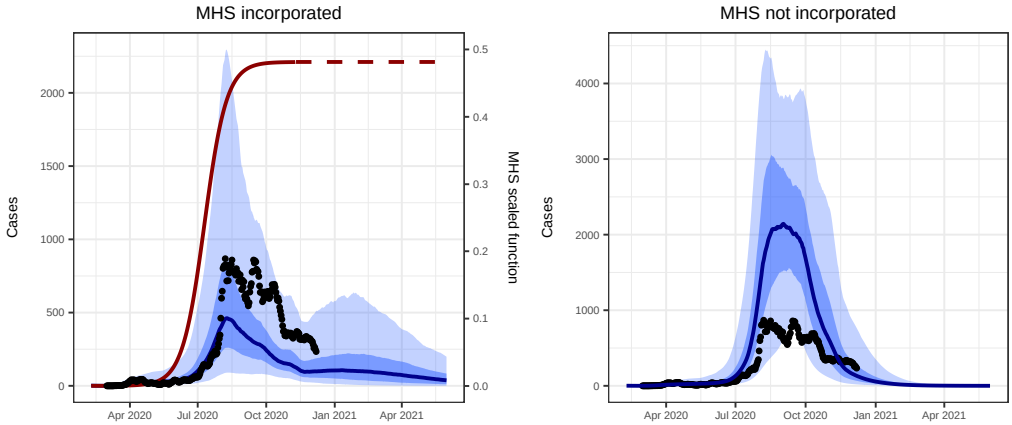

Figure 5 – Comparison of models that included and did not include Minimum Health Standards (MHS) with daily confirmed cases for Calabarzon. We calibrated the Calabarzon model to daily confirmed cases (black dots; same in both plots with different y-axes), which included MHS (left) and ran a counterfactual scenario that did not include MHS (right). Each plot shows the median modeled detected cases (blue line) with shaded areas representing the 25th to 75th centile (dark blue) and 2·5th to 97·5th centile (light blue) of estimated detected cases. The red curve represents the effect of MHS (i.e., reduced transmission risk per contact) in the model through time. The MHS effect value is squared in the model to account for the reduction in the probability of an infected person passing on the infection and the probability of a contact being infected, prior to adjustment of each cell of the mixing matrix.

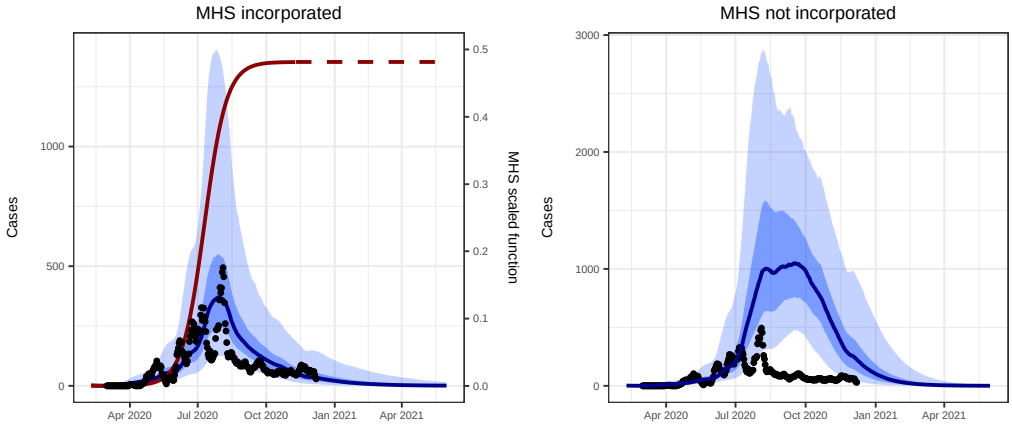

Figure 6 – Comparison of models that included and did not include Minimum Health Standards (MHS) with daily confirmed cases for Central Visayas. We calibrated the Central Visayas model to daily confirmed cases (black dots; same in both plots with different y-axes), which included MHS (left) and ran a counterfactual scenario that did not include MHS (right). Each plot shows the median modeled detected cases (blue line) with shaded areas representing the 25th to 75th centile (dark blue) and 2·5th to 97·5th centile (light blue) of estimated detected cases. The red curve represents the effect of MHS (i.e., reduced transmission risk per contact) in the model through time. The MHS effect value is squared in the model to account for the reduction in the probability of an infected person passing on the infection and the probability of a contact being infected, prior to adjustment of each cell of the mixing matrix.

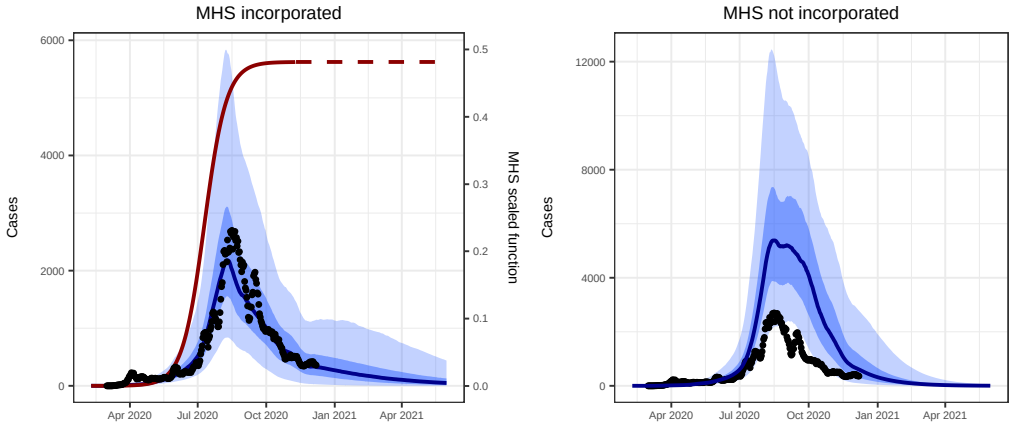

Figure 7 – Comparison of models that included and did not include Minimum Health Standards (MHS) with daily confirmed cases for the National Capital Region. We calibrated the National Capital Region model to daily confirmed cases (black dots; same in both plots with different y-axes), which included MHS (left) and ran a counterfactual scenario that did not include MHS (right). Each plot shows the median modeled detected cases (blue line) with shaded areas representing the 25th to 75th centile (dark blue) and 2·5th to 97·5th centile (light blue) of estimated detected cases. The red curve represents the effect of MHS (i.e., reduced transmission risk per contact) in the model through time. The MHS effect value is squared in the model to account for the reduction in the probability of an infected person passing on the infection and the probability of a contact being infected, prior to adjustment of each cell of the mixing matrix.

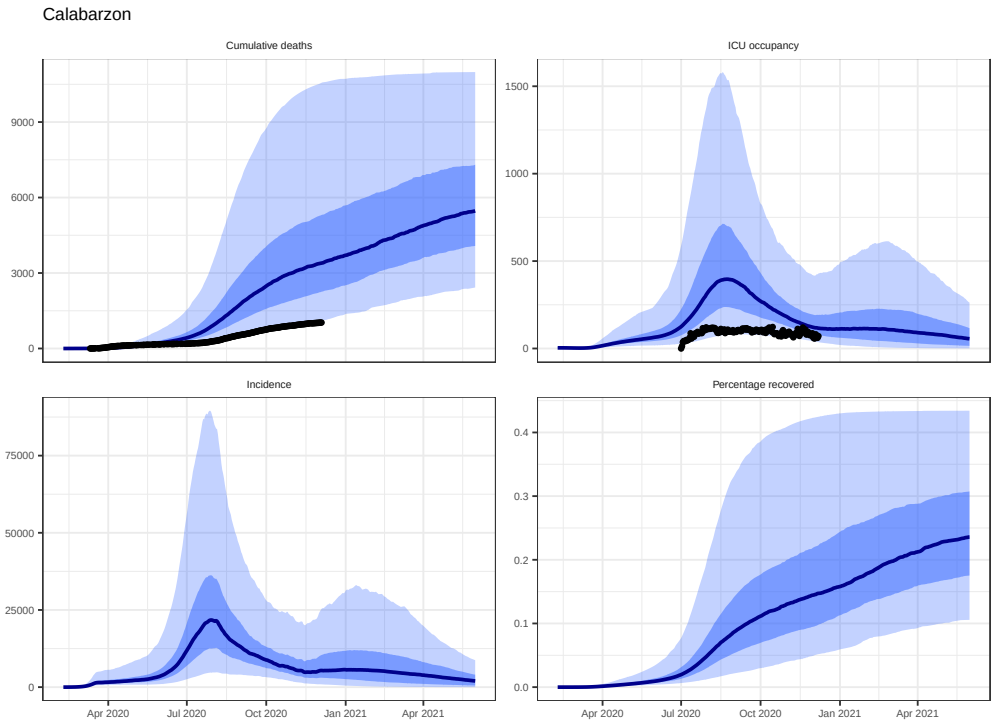

Figure 8 – Model estimated epidemic indices from the calibrated Calabarzon model. Modeled median cumulative deaths, ICU occupancy, incidence, and percentage of the population recovered from COVID-19 (blue line) with shaded areas for 25th to 75th centile (dark blue) and 2·5th to 97·5th centile (light blue) and overlaid with reported cumulative deaths and ICU occupancy (black dots).

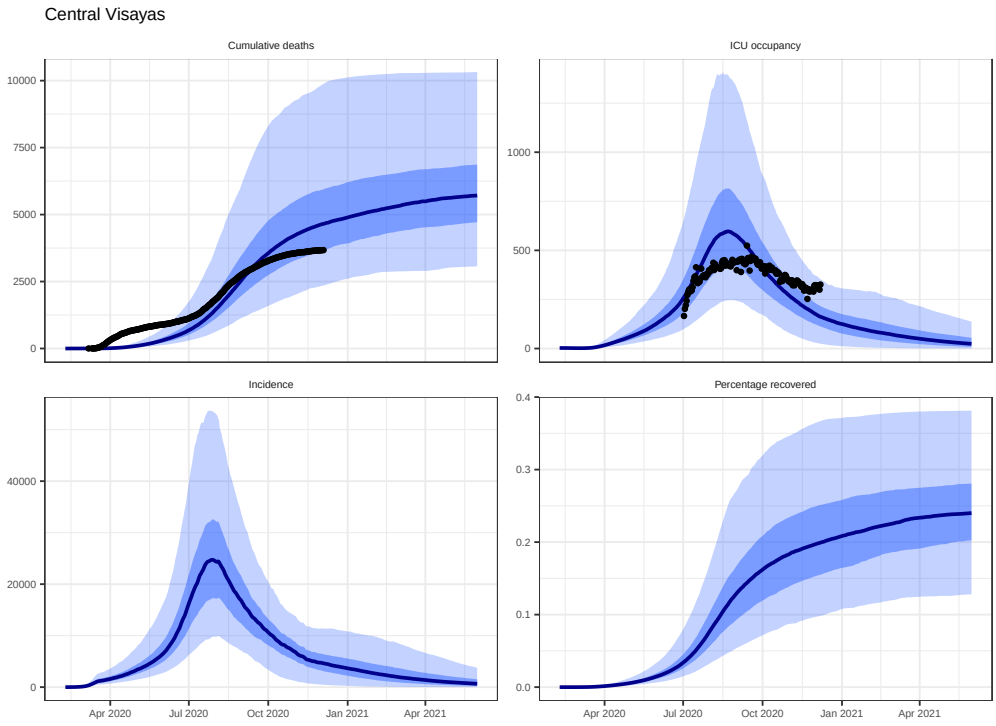

Figure 9 – Model estimated epidemic indices from the calibrated Central Visayas model. Modeled median cumulative deaths, ICU occupancy, incidence, and percentage of the population recovered from COVID-19 (blue line) with shaded areas for 25th to 75th centile (dark blue) and 2·5th to 97·5th centile (light blue) and overlaid with reported cumulative deaths and ICU occupancy (black dots).

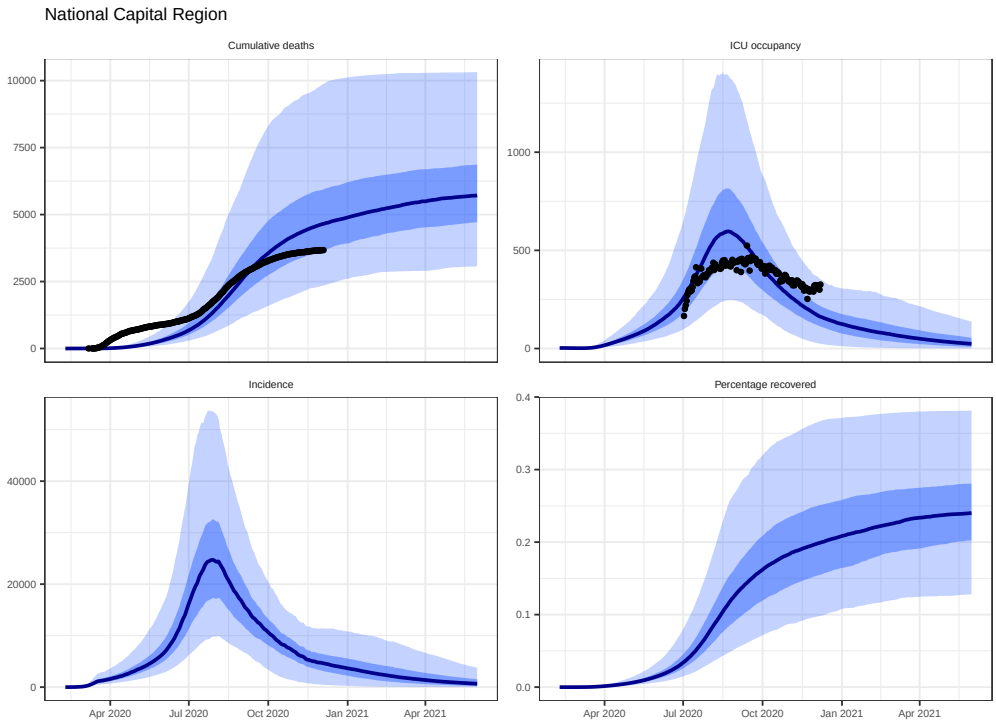

Figure 10 – Model estimated epidemic indices from the calibrated National Capital Region model. Modeled median cumulative deaths, ICU occupancy, incidence, and percentage of the population recovered from COVID-19 (blue line) with shaded areas for 25th to 75th centile (dark blue) and 2·5th to 97·5th centile (light blue) and overlaid with reported cumulative deaths and ICU occupancy (black dots).

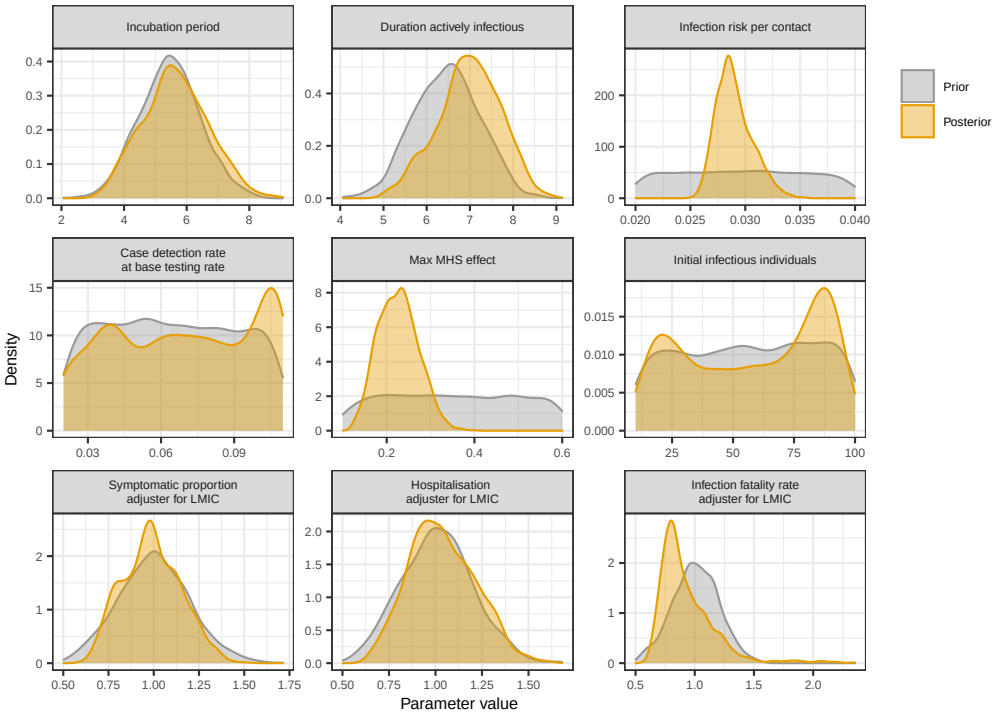

Figure 11 – Histograms of prior and posterior epidemiological parameter distributions for the Philippines national model. MHS refers to Minimum Health Standards. All parameters with the term "adjuster" allow for modification to the best estimates from the literature (i.e., the priors). The parameter value of the posterior provides the odds ratio used in the model to adjust the odds of an event. For example, "infection fatality rate" was adjusted downwards in the majority of the posterior probability distribution, but adjusted upwards as much as 1·5-1·75 fold in a small minority.

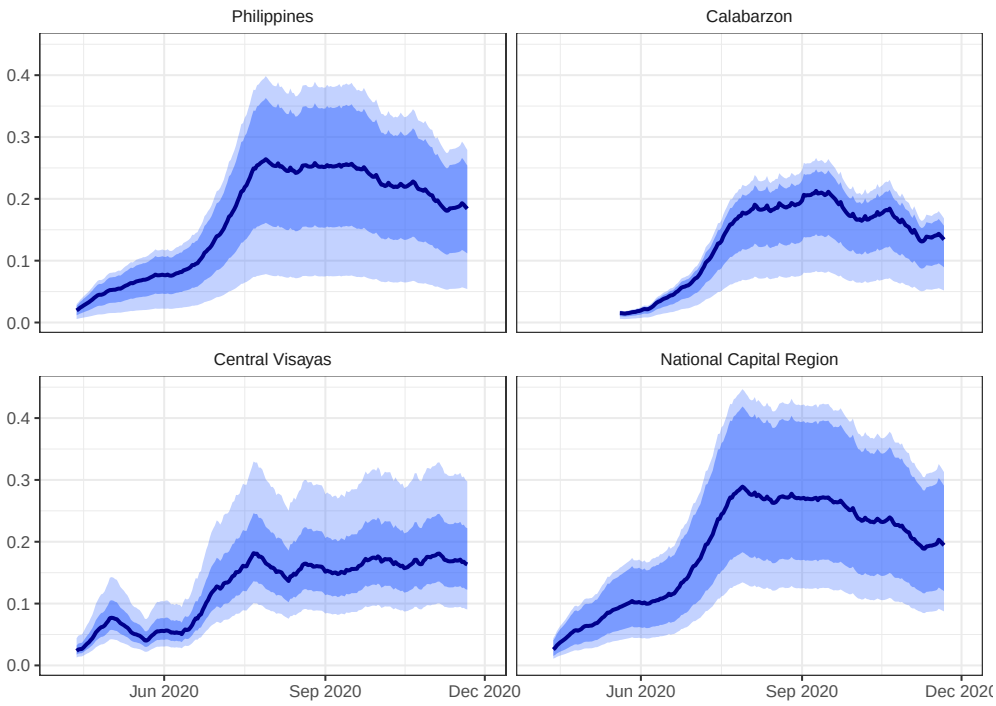

Figure 12 – Model estimated case detection rates varied across regions and through time, peaking at ¡50%. We derived values for the symptomatic cases detected through time from the daily number of tests performed, the population size, and the calibrated parameter representing the value of the case detection rate given a testing rate of one test per 10,000 persons per day. We provide a list of laboratory facilities that conducted tests in the three regional models in Table S1.

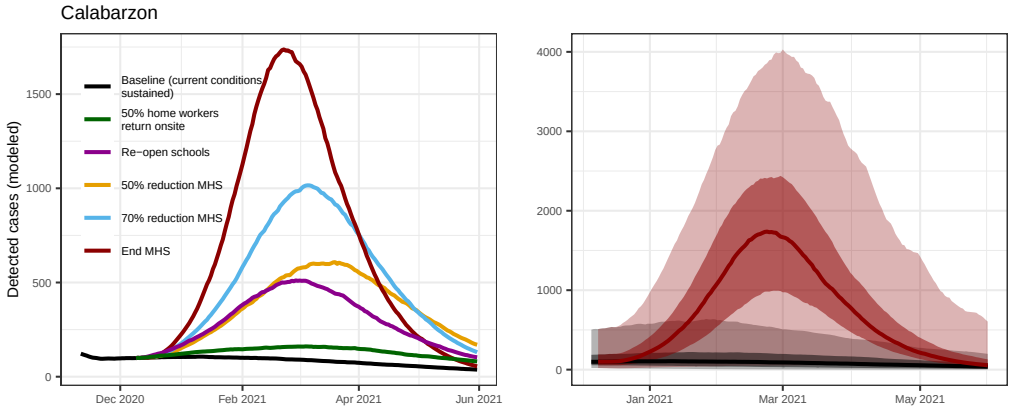

Figure 13 – Epidemic scenario projections for Calabarzon. Median estimates of daily confirmed cases expected under different policy changes (left). Median estimates of daily confirmed cases (lines) with 25th to 75th centiles (dark shading) and 2·5th to 97·5th centiles (light shading) for the baseline scenario (where current conditions are carried forward) and for the scenario where MHS policy ends. Note the different y-axes on each plot.

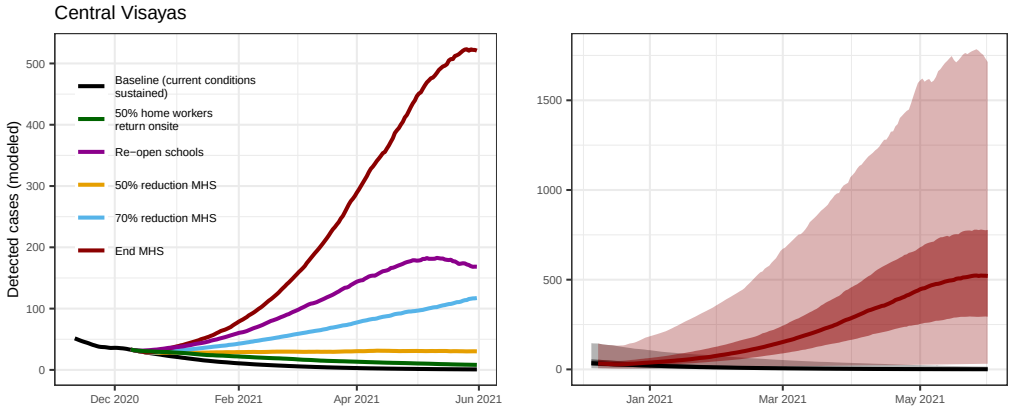

Figure 14 – Epidemic scenario projections for Central Visayas. Median estimates of daily confirmed cases expected under different policy changes (left). Median estimates of daily confirmed cases (lines) with 25th to 75th centiles (dark shading) and 2·5th to 97·5th centiles (light shading) for the baseline scenario (where current conditions are carried forward) and for the scenario where MHS policy ends. Note the different y-axes on each plot.

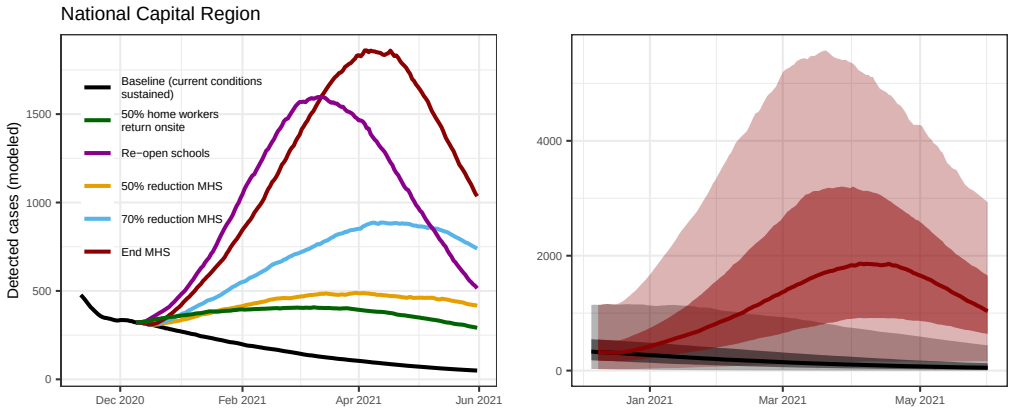

Figure 15 – Epidemic scenario projections for the National Capital Region. Median estimates of daily confirmed cases expected under different policy changes (left). Median estimates of daily confirmed cases (lines) with 25th to 75th centiles (dark shading) and 2·5th to 97·5th centiles (light shading) for the baseline scenario (where current conditions are carried forward) and for the scenario where MHS policy ends. Note the different y-axes on each plot.

References

[1] J. M. Trauer et al. Modular programming for tuberculosis control, the "AuTuMN" platform. *BMC Infectious Diseases*, 17(1):546, dec 2017.

[2] C. G. McAloon et al. The incubation period of COVID-19: A rapid systematic review and meta-analysis of observational research. Technical Report 8, aug 2020.

[3] K. Prem et al. Projecting social contact matrices in 152 countries using contact surveys and demographic data. *PLoS Computational Biology*, 13(9):e1005697, sep 2017.

[4] M. O'Driscoll et al. Age-specific mortality and immunity patterns of SARS-CoV-2. *Nature*, nov 2020.

[5] J. Zhang et al. Evolving epidemiology and transmission dynamics of coronavirus disease 2019 outside Hubei province, China: a descriptive and modelling study. *The Lancet Infectious Diseases*, 20(7), 2020.

[6] S. A. Lauer et al. The Incubation Period of Coronavirus Disease 2019 (COVID-19) From Publicly Reported Confirmed Cases: Estimation and Application. *Annals of Internal Medicine*, 172(9):577–582, may 2020.

[7] Q. Li et al. Early transmission dynamics in Wuhan, China, of novel coronavirus-infected pneumonia, mar 2020.

[8] Q. Bi et al. Epidemiology and Transmission of COVID-19 in Shenzhen China: Analysis of 391 cases and 1,286 of their close contacts. *medRxiv*, pp. 2020.03.03.20028423, mar 2020.

[9] M. T. Meehan et al. Modelling insights into the COVID-19 pandemic, jun 2020.

[10] X. He et al. Temporal dynamics in viral shedding and transmissibility of COVID-19. *Nature Medicine*, pp. 2020.03.15.20036707, mar 2020.

[11] A. W. Byrne et al. Inferred duration of infectious period of SARS-CoV-2: rapid scoping review and analysis of available evidence for asymptomatic and symptomatic COVID-19 cases. *BMJ open*, 10(8):e039856, aug 2020.

[12] M. Pritchard et al. ISARIC Clinical Data Report 4 October 2020. *medRxiv*, pp. 2020.07.17.20155218, jan 2020.

[13] ISARIC. ISARIC (International Severe Acute Respiratory and Emerging Infections Consortium) COVID-19 Report: 08 June 2020. Technical report, 2020.

[14] N. G. Davies et al. Age-dependent effects in the transmission and control of COVID-19 epidemics. *Nature Medicine*, pp. 2020.03.24.20043018, may 2020.

[15] J. Zhang et al. Changes in contact patterns shape the dynamics of the COVID-19 outbreak in China. *Science*, 368(6498):1481–1486, jun 2020.

[16] M. Pollán et al. Prevalence of SARS-CoV-2 in Spain (ENE-COVID): a nationwide, population-based seroepidemiological study. *Lancet (London, England)*, 0(0), jul 2020.

[17] Epidemiologische situatie COVID-19 in Nederland. Technical report.

[18] H. Haario et al. An adaptive Metropolis algorithm. *Bernoulli*, 2001.